Viser Technology Pte. Ltd.
Research and Application of Materials Science
DOI: 10.33142/rams.v3i2.6730

Research Article Open Access

Influence of Mn and Mg Contents on Mechanical Properties of the Die-casting Aluminum Alloy HL-111

Yanyang HE*, Gang XU, Xiguang YU

Ningbo Heli Mould Technology Co., Ltd. Ningbo, Zhejiang, China

***Corresponding Author:** Yanyang HE, Ningbo Heli Mould Technology Co., Ltd. Ningbo, Zhejiang, China; yanyang.he@Helimould.com*

Abstract:
In this study, four groups of thin plate samples with a wall thickness of 2.2mm, 2.5mm, 2.7mm, and 3.0mm are prepared by ultra-high vacuum die casting. The effects of Mn, Mg, and Mn/Mg ratio on the microstructure and mechanical properties of samples with different wall thicknesses are obtained by different test and analysis methods. The results show that as the content of Mn is 0.4% ～ 0.65%, the content of Mg is 0.17% ～ 0.5%, and the Mn / Mg ratio reaches 1.69 ～ 1.90, the tensile strength, yield strength, and elongation of HL-111 alloy with a wall thickness of 2 ～ 3mm can reach more than 280MPa, 120MPa and 10% respectively, and the mechanical properties of the material are greatly improved. In addition, the tensile strength, yield strength, and elongation of HL-111 alloy after T5 heat treatment at 165℃ for 510min reach 302.36 MPa, 190.32 MPa, and 8.42%. The precipitated phase of Mg_2Si leads to changes in strength and elongation.
Keywords: *HL-111 alloy; Mn/Mg element ratio; Microstructure; Mechanical properties*

1 Introduction

Al-Si alloys (such as Magcimal-59, Castasil-37, and Silafont-36) are widely used in ultra-high vacuum and high-pressure casting of conventional parts because of their good casting properties [1]. With the continuous improvement of automobile lightweight technology, Silafont-36 alloy has high strength and elongation, which is particularly favored in the manufacture of structural parts with high requirements for safety performance, such as car body frame and shock absorber [2-3]. Especially, the continuous innovation of ultra-high vacuum pressure casting technology, the increasing maturity of large die casting machine technology, and the needs of new energy vehicles make Silafont-36 alloy shine in the application of die casting large-size, complex structure, and ultra-thin wall thickness structural parts [4-6].

Due to the large size and complex structure of structural body parts, they usually have extremely high requirements for wall thickness. Take the application of Silafont-36 alloy in the shock tower as an example, its functional area wall thickness is in the range of 2～3 mm. However, Silafont-36 alloy is usually subjected to T7 heat treatment during the high-pressure casting production process in order to ensure the high strength and high toughness of the structural parts, which is prone to different degrees of unpredictable deformation after the T7 heat treatment, and the resulting rework correction and scrap rate are great costs. At the same time, T7 heat treatment will also make the production costs significantly increased. These increases of upstream manufacturing cost will aggravate the improvement of downstream industry cost, which will lead to the enterprise being invisible in the heavy burden forward. Therefore, it is imperative to find a way to maintain the high toughness and high strength of Silafont-36 alloy after die-casting, so as to reduce the manufacturing cost by eliminating the T7 heat treatment.

The main methods to improve the strength of the alloy mainly include fine-grain strengthening, dispersion strengthening, etc. Therefore, the strength of the alloy can be improved by controlling the strengthening phase in the alloy. It is well known that Mg_2Si is a common strengthening phase in aluminum alloys because of its high strength, but when the magnesium element is excessive, it will cause the coarsening of the Mg_2Si phase, which will reduce the strength of the alloy, so reasonable control of the magnesium element content in the alloy will be beneficial to enhance the strength of the alloy. On the contrary, the dispersion strengthening of Mg_2Si can improve the strength of the alloy, but it will also reduce the plasticity and toughness of the alloy, so we should take measures to improve the plasticity and toughness of the alloy at the same time. One of the most effective methods is to refine the grain of the alloy. Manganese is one of the strengthening elements of aluminum alloy, which can reduce the size of recrystallized grains and

Received on October 20, 2021; Accepted on December 26, 2021

improve the strength, plasticity, and toughness of the alloy. Therefore, proper adjustment of the Mn/Mg element ratio in the alloy can achieve the purpose of improving the strength and toughness of the alloy at the same time to replace the T7 heat treatment.

Ningbo Heli Technology Co., Ltd. has several years of practical production experience in the die-casting Silafont-36 alloy, focusing on the improvement of part qualification rate and the control of production cost. Based on Silafont-36, the company has reasonably allocated alloy elements and obtained an HL-111 alloy product with different wall thicknesses. The as-cast mechanical properties of HL-111 alloy fully meet the requirements of high strength and high toughness of the original Silafont-36 alloy after T7 heat treatment, which can omit the T7 heat treatment process of parts and eliminate all costs brought by the whole process.

2 Experimental

The molten aluminum was melted in a 300 kg resistance furnace. When the temperature was set at 720℃, the refining degassing time was 50 min. In the degassing process, the modifier Al-10Sr master alloy [7-8] and super refiner TCB seed alloy [9-10] were added, during which the degassing was uninterrupted. After the refining degassing was qualified, stand for 10 min, and transferred the molten aluminum to the side furnace of 300T-Buhler small die casting machine after the temperature of the molten aluminum was stabilized at 710℃. Then HL-111 die casting samples with a wall thickness of 2.2 mm, 2.5 mm, 2.7 mm, and 3 mm and corresponding element ratio were carried out successively, the physical drawing of the casting is shown in Figure 1. After the preparation of castings, HL-111 die-casting samples were prepared by wire cutting according to the requirements of GB / T 228 standard. After that, the HL-111 die-casting samples with the best performance were selected and subjected to T5 heat treatment at 155℃, 165℃, and 175℃ for 120 min, 240 min, and 510 min respectively to obtain HL-111 heat-treated samples.

Figure 1 The physical drawing of HL-111 casting

During the test, the alloy chemical composition of the HL-111 die-casting sample was analyzed by SPECTRO MAXx07-F element direct reading spectrometer. Wipe the sample surface and the spark table of the direct-reading spectrometer with absolute ethanol to avoid impurities affecting the analysis results. Select the brand of Silafont-36 alloy for spectral analysis. Combined with the actual element percentage of four Mn/Mg ratio levels, the element composition was obtained when the alloy wall thickness was 2 ～ 3 mm, as shown in Table 1.

Table 1 Table of optimum alloy elements with a wall thickness of 2 ～ 3mm

Element	Si	Fe	Mn	Mg	Cu
Count (%)	9.5～11.5	≤0.15	0.4～0.65	0.17～0.5	＜0.05
Element	Sr	Zn	Ti	Other	Al
Count (%)	0.02～0.03	0.07～0.1	≤0.2	＜0.15	Other

CMT5205 electronic universal testing machine was used to carry out the tensile test on two kinds of samples to measure their mechanical properties. The microstructure of the sample was analyzed by OLYMPUS GX53 metallographic microscope and scanning electron microscope (SEM, Nova SU-70, Hitachi). The metallographic diagrams of Silafont-36 alloy and HL-111 alloy with different wall thickness can be seen in Figure 2. The transmission electron microscope samples of HL-111 alloy were prepared by Gatan 695 ion thinning instrument. The transmission electron microscope patterns of HL-111 alloy were measured by FEI Talos F200X.

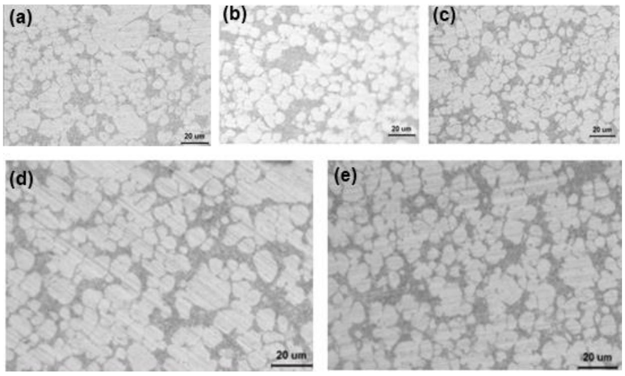

Figure 2 (a) Metallographic diagram of Silafont-36 alloy. (b-e) Metallographic diagram of HL-111 sample with a wall thickness of 2.2 mm (b), 2.5 mm (c), 2.7 mm (d), and 3.0 mm (e)

Table 2 The number of HL-111 die casting samples

Num	Wall thickness (mm)	Mn/Mg
1		1.65
…	2.2	
12		1.90
13		1.65
…	2.5	…
24		1.90
25		1.65
…	2.8	…
36		1.90
37		1.65
…	3.0	…
48		1.90

Tensile test design of HL-111 die-casting specimen: adopting four kinds of die-casting specimens with a length of 200 mm, a width of 40 mm, and thickness of 2.2 mm, 2.5 mm, 2.8 mm, and 3.0 mm. The Mn/Mg ratio of the specimens with different thicknesses is adjusted to 1.65, 1.69, 1.71, 1.73, 1.75, 1.77, 1.79, 1.81, 1.83, 1.85, 1.88, and 1.90 respectively, and the serial numbers are numbered 1, 2, 3..., 47 and 48, as shown in Table 2.

3 Results and Discussions

3.1 Analysis of chemical composition and microstructure of HL-111 alloy

The microstructure of the sample was analyzed by 500X optical microscope. During the crystallization process of Silafont-36 alloy, α_1-Al phase will be precipitated first, and the liquid aluminum alloy reaches aluminum-silicon eutectic composition. As the temperature decreases, the eutectic silicon phase in the liquid alloy will grow coupled with α_2-Al phase until complete solidification. As shown in Figure 2a, it can be seen that in the as-cast structure of the original Silafont-36 alloy, the white coarser organization is the primary α_1-Al phase. The fine and round white structure is the secondary α_2-Al phase. The irregular growth of the α-Al phase can inhibit the growth of the eutectic silicon phase and thus constantly change the growth direction, which eventually generates relatively closed clusters [11-13], which reduces the coupling degree with other phases. The length of the α_1-Al phase is greater than 27.09 μm, the diameter of α_2-Al phase is 7.41 μm, the proportion of eutectic silicon is 36.91%. This non-uniform distributed organization will lead to uneven stress distribution in the process of stressing the alloy, causing damage to the weak phases in the alloy and reducing the overall mechanical properties.

By comparing the microstructure distribution differences between HL-111 die-casting specimens with four different wall thicknesses and the original silafont-36 alloy, Figure 2b-d indicated that as the Mn / Mg ratio reached the range of 1.73 ～ 1.89, the primary phase and second phase of α-Al were not obvious. In addition, the eutectic silicon was fully coupled to grow, and the overall distribution was relatively uniform, which is conducive to enhancing the toughness and strength of HL-111 alloy. The size of the α-Al phase was calculated by the software, the maximum length of the α_1-Al phase was only 16.43 μm, the diameter of the secondary phase was 7.40 μm, and the percentage of eutectic silicon was reduced to 26.62% ～ 30.02%.

Mg_2Si phase will precipitate after T5 heat treatment at 165℃ for 510 min in the HL-111 die-casting sample. Firstly, the element distribution of the ion milling sample is analyzed by X-ray energy dispersive spectrometer (EDS) through the transmission electron microscope (TEM), as shown in Figure 3a. The yellow area in the figure is the possible location of the precipitated phase. Then, implementing spot measurement to the yellow area by EDS of TME to further determine the location of the Mg_2Si precipitated phase, as shown in Figure 3a, b. To further prove that there was precipitation of Mg_2Si phase in the HL-111 sample after T5 heat treatment, the area circled in Figure 3a is analyzed by selected-area electron diffraction and high-resolution transmission electron microscope (HRTEM). By calibrating the diffraction pattern and lattice spacing of the precipitated phase (Figure 3e, f), it is completely consistent with the PDF card (#65-9365) of Mg_2Si, which fully demonstrated that the Mg_2Si phase was precipitated after T5 heat treatment of HL-111. The morphology of Mg_2Si is shown in Figure 3c, d. Through the analysis of the Mg_2Si precipitated phase and its surrounding elements by high-angle annular dark-field (HAADF), there were evenly dispersed aluminum atoms around Mg_2Si precipitated phase, indicating that the precipitated phase is distributed on Al substrate. The Mg_2Si phase could hinder the dislocation movement and was conducive to improving the yield strength of HL-111 alloy, as shown in Figure 3g-j.

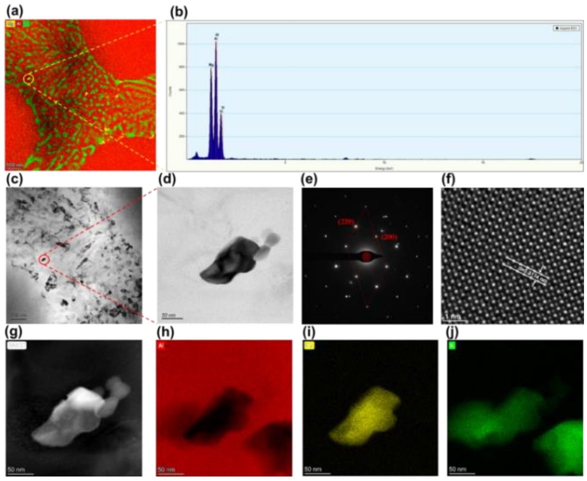

Figure 3 (a) The EDS mapping of HL-111alloy. (b) EDS point measurement in the area within the yellow circle. (c) TEM image of HL-111 after T5 heat treatment. (d) TEM morphology of Mg_2Si precipitated phase. (e) Selected-area electron diffraction (SAED) pattern of Mg_2Si precipitated phase. (f) The HRTEM image of Mg_2Si. (g-j) The HAADF diagram (g) and element distribution diagram of Mg_2Si precipitated phase: Al element (h), Mg (i), and (Si).

3.2 Mechanical property test

The dimensions of tensile specimens are shown in Figure 4. The operation and parameters of the tensile experiment are as follows. Remove the oil stain from the surface of the standard specimen. Set the test parameters of the universal testing machine according to GB/T228 standard [14]: the tensile speed was 4 mm/s, the extensometer was YYU-10/50, then input the cross-sectional area of the sample, and the tensile test is carried out. The tensile test results of HL-111 die-casting samples with different wall thicknesses are shown in Table 3 The tensile test results of the HL-111 sample with a wall thickness of 2.7 mm after different T5 heat treatments are shown in Table 4.

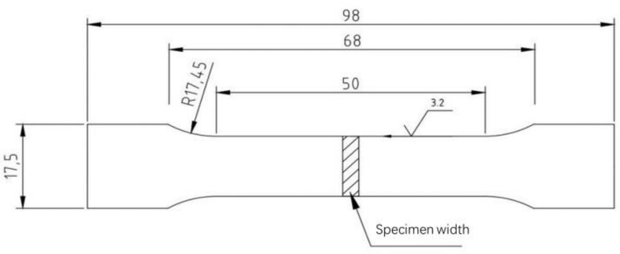

Figure 4 Schematic diagram of tensile specimen

Table 3 The mechanical properties of HL-111 die-casting samples with different wall thickness

Specimen thickness (mm)	Tensile strength (MPa)	Yield strength (MPa)	Elongation (%)
2.2	284.58	122.21	11.06
2.2	288.82	124.4	11.77
2.5	287.82	127.25	10.67
2.5	280.14	120.05	12.43
2.7	291.04	129.86	11.93
2.7	283.93	122.92	10.34
3	295.14	123.83	11.24
3	299.21	125.72	10.4

Table 4 The mechanical properties of HL-111 after different T5 heat treatments

Heat treatment parameters (℃/min)	Tensile strength (MPa)	Yield strength (MPa)	Elongation (%)
155℃/120min	294.05	182.30	5.84%
155℃/240min	296.34	184.52	5.63%
155℃/510min	299.50	188.47	5.72%
165℃/120min	295.28	184.23	5.76%
165℃/240min	297.44	186.48	5.83%
165℃/510min	302.36	190.32	8.42%
175℃/120min	296.32	186.23	5.53%
175℃/240min	299.62	189.24	5.73%
175℃/510min	305.32	192.93	5.62%

The elongation of the original Silafont-36 alloy after T7 heat treatment is generally 10%, the tensile strength is 200 MPa, and the yield strength is 120 MPa. As can be seen from Table 3, controlling the relationship between wall thickness and composition, the elongation of HL-111 as-cast samples without heat treatment exceeded 10% and the yield strength was stable above 120 MPa. More importantly, the tensile strength was significantly improved and could reach more than 280 MPa. According to the Hall-Petch formula, with the decrease of grain size, the number of large-angle grain boundaries of the alloy will increase [15]. When the alloy is subjected to external stress, the dislocations in the grain cannot cross the grain boundary and accumulate on it. When the external stress increases, the dislocation source of adjacent grains will move and start plastic deformation [16]. Therefore, HL-111 alloy with smaller grains would have a greater strength [17]. At the same time, the grain distribution of HL-111 alloy was more uniform. When the alloy had plastic deformation, the plastic deformation could be more evenly distributed in each grain, which was not easy to produce stress concentration, so HL-111 alloy could withstand more deformation and have a good plasticity. Compared with Silafont-36, the proportion of eutectic silicon in HL-111 is reduced. The reduction of the proportion of eutectic silicon can not only reduce the strength reduction caused by eutectic silicon but also improve the yield strength of HL-111 alloy.

After T5 heat treatment at 165℃ for 510 min, the tensile strength of HL-111 was 290-310 MPa, the yield strength was 180-220 MPa, and the elongation was higher than 8%, while the elongation after heat treatment at other temperature and time was less than 6%. Because the HL-111 alloy will precipitate the Mg_2Si phase at the grain boundary after T5 heat treatment at 165 ℃ for 510min. The precipitation of Mg_2Si phase would form Cottrell atmosphere at the grain boundary and lead to the pinning effect, which could hinder the dislocation slip in the HL-111 alloy and increase the strength of the metal, especially the yield strength. Moreover, the yield ratio of HL-111 alloy will also increase, which will make the metal difficult to plastic deformation, which will lead to the decrease of elongation. The time and temperature of heat treatment will affect the precipitation and distribution of Mg_2Si. When the heat treatment time is too long or short, the plasticity of HL-111 will significantly decrease.

3.3 Fracture dimple analysis

The fracture morphology of the original Silafont-36 alloy is shown in Figure 5a, b, and the fracture morphology of the HL-111 sample after adjusting the Mn/Mg ratio is shown in Figure 5c-h. The size of the fracture dimples mainly includes the average size and depth, which is closely related to the plasticity and fracture mode of the material. The parts with deeper fracture dimples break later in the fracture process, so the aluminum alloy with deeper fracture dimples has better plasticity. By comparing the dimple size of HL-111 alloy with different wall thickness and the original Silafont-36 alloy, as Mn/Mg reaches the range of 1.73-1.89, the dimple size and number of the HL-111 alloy are larger than Silafont-36 alloy. Therefore, the HL-111 alloy has excellent plasticity, and the elongation can reach more than 10%. This is because the proportion of eutectic silicon decreases while the α-Al phase increases after adjusting the Mn/Mg ratio, and brittle fracture occurs first at the eutectic silicon during the tensile process, however, the increase of α-Al phase can increase the plasticity of the HL-111 alloy.

After T5 heat treatment, the dimple size and depth on the fracture surface of HL-111 alloy become smaller, and the fracture surface locally presents the rock shape with a few tear lines, which shows the plasticity of the T5 heat-treated HL-111 alloy is less than that of as-cast alloy [18]. The fracture mode of T5 heat-treated HL-111 alloy in the tensile test is between brittle fracture and ductile fracture. Because the Mg_2Si precipitated from HL-111 alloy after heat treatment is brittle and distributes on the grain boundary. Under the action of stress, there will be some microporous cracks, which make the alloy brittle.

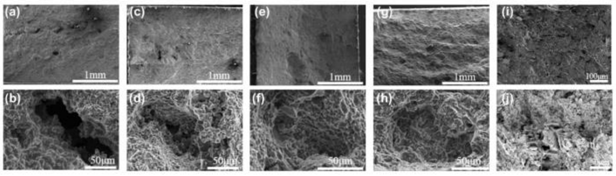

Figure 5 The SEM images of the fracture surface of Silafont-36, HL-111 with different wall thickness and T5 heat-treated HL-111 alloy. (a-b) Tensile fracture morphology of Silafont-36 as-cast alloy; (c-h) Tensile fracture morphology of HL-111 alloy die-casting specimen. (i-j) Tensile fracture morphology of HL-111 sample after T5 heat treatment(165℃/510min)

4 Conclusion

Based on the element content of the Silafont-36 alloy, the tensile strength, yield strength, and elongation of HL-111 alloy with different wall thickness can reach more than 280 MPa, 120 MPa, and 10% respectively by adjusting Mn/Mg ratio. More importantly, as the Mn/Mg ratio reaches 1.73 ～ 1.89, the as-cast HL-111 alloy with a wall thickness of 2-3 nm can replace the T7 heat treatment process of the original Silafont-36 alloy. In addition, as the Mn/Mg ratio in HL-111 is 1.73 ～ 1.89, the crystallization law of microstructure in HL-111 will change. The distance between the primary phase and the secondary phase of α-Al decreases, and the grains are regularly and evenly distributed, to better improve the mechanical properties of the alloy. Moreover, Mg_2Si will precipitate in HL-111 alloy after T5 heat treatment at 165℃ for 510 min and distribute on the grain boundary, which will produce a pinning effect to improve the metal strength, and slightly reduce the elongation. The tensile strength, yield strength, and elongation of HL-111 alloy after T5 heat treatment with 2.7 mm wall thickness can reach 302.36 MPa, 190.32 MPa, and 8.42%.

Author Contributions: YH put forward the experimental idea and designed the experiment, analyzed the data, and finally wrote the draft of the article. GX and XY also implemented some experimental tests and revised the original draft. All authors read and approved the final manuscript.

Conflict of Interest: The authors declare that there is no conflict of interest regarding the publication of this paper.

References

[1] Cai Z, Zhang C, Wang R, et al., Preparation of Al－Si alloys by a rapid solidification and powder metallurgy route. Mater. Des, 2015(87): 996-1002.

[2] Dash S S, Li D J, Zeng X Q, et al., Heterogeneous microstructure and deformation behavior of an automotive grade aluminum alloy. Alloys Compd, 2021, 870: 159413.

[3] Meschut G, Matzke M, Hoerhold R, et al., Hybrid Technologies for Joining Ultra-high-strength Boron Steels with Aluminum Alloys for Lightweight Car Body Structures. Procedia CIRP, 2014(23): 19-23.

[4] Jiao X Y, Zhang Y F, Wang J, et al., Characterization of externally solidified crystals in a high-pressure die-cast AlSi10MnMg alloy and their effect on porosities and mechanical properties. J Mater Sci Technol 2021, 298: 117299.

[5] Dou K, Lordan E, Zhang Y, et al., A novel approach to optimize mechanical properties for aluminium alloy in High pressure die casting (HPDC) process combining experiment and modelling. J Mater Sci Technol, 2021, 296: 117193.

[6] Liu R, Zheng J, Godlewski L, et al., Influence of pore characteristics and eutectic particles on the tensile properties of Al–Si–Mn–Mg high pressure die casting alloy. Mater. Sci. Eng. A, 2020, 783: 139280.

[7] Qiu K, Wang R C., Peng C Q, et al., Effect of individual and combined additions of Al–5Ti–B, Mn and Sn on sliding wear behavior of A356 alloy. Trans. Nonferrous Met. Soc. China 2015, 25, 3886-3892.

[8] Tan P , Yang Y, Sui Y, et al., The influence of Al–10Sr or/and Al－5Ti–1B on microstructure and mechanical properties of Al–12Si–4Cu–2Ni–0.8 Mg alloys. J.Alloys Compd, 2019, 809: 151856.

[9] Li P, Liu S, Zhang L, Liu X. Grain refinement of A356 alloy by Al–Ti–B–C master alloy and its effect on mechanical properties. Mater. Des 2013, 47, 522-528.

[10] Zhao K, Gao T, Yang H, et al., Influence of a new AlTiC–B master alloy on the casting and extruding behaviors of 7050 alloys. J. Alloys Compd 2020, 820: 153089.

[11] Wang J, Guo Z, Song J L, et al., On the growth mechanism of the primary silicon particle in a hypereutectic Al-20 wt%Si alloy using synchrotron X-ray tomography. Mater. Des 2018, 137, 176-183.

[12] Wang S R, Ma R, Wang Y Z, et al., Growth mechanism of primary silicon in cast hypoeutectic Al-Si alloys. Trans. Nonferrous Met. Soc. China 2012, 22, 1264-1269.

[13] Fang N, Zou C, Wei Z, et al., Microstructural evolution and mechanical properties of Al–Si–Cu–(Ge)–(Mg) alloy solidified under high pressure. Mater. Sci. Eng. A 2021, 827: 142065.

[14] Xiao Y, Hu Y. Numerical and Experimental Fracture Study for 7003 Aluminum Alloy at Different Triaxialities. Met.Mater. Int 2020, 27, 2499-2511.

[15] Naik S N, Walley S M. The Hall–Petch and inverse Hall–Petch relations and the hardness of nanocrystalline metals. J. Mater. Sci 2019, 55, 2661-2681.

[16] Loucif A, Figueiredo R B, Baudin T, et al., Ultrafine grains and the Hall–Petch relationship in an Al–Mg–Si alloy processed by high-pressure torsion. Mater. Sci. Eng. A 2012, 532, 139-145.

[17] Liu L, Zhang Y, Han J, et al., Nanoprecipitate-Strengthened High-Entropy Alloys. Adv Sci (Weinh) 2021, 8: e2100870.

[18] Suryanarayana C, Al-Aqeeli N. Mechanically alloyed nanocomposites. Prog. Mater. Sci. 2013, 58, 383-502.